

## MEASUREMENTS AT THE ALICE TOMOGRAPHY SECTION\*

M.G. Ibison<sup>#1,2</sup>, K.M. Hock<sup>1,2</sup>, D.J. Holder<sup>1,2</sup>, M. Korostelev<sup>1,2</sup>, B.D. Muratori<sup>3,2</sup>, and A. Wolski<sup>1,2</sup>

<sup>1</sup>Department of Physics, University of Liverpool, Liverpool L69 7ZE, United Kingdom

<sup>2</sup>Cockcroft Institute, Daresbury Laboratory, Warrington WA4 4AD, United Kingdom

<sup>3</sup>ASTeC, STFC, Daresbury Laboratory, Warrington WA4 4AD, United Kingdom

### Abstract

This paper reports the results of tomography measurements of the electron beam transverse phase space distribution in the ALICE accelerator at Daresbury Laboratory. These measurements have two main aims. The first is to give a detailed picture of the phase space distribution of the electron beam injected from ALICE into the EMMA prototype non-scaling FFAG accelerator. The second is to provide data for the development and testing of a variety of techniques for tomographic reconstruction. We summarise the measurement results which we have obtained and discuss the advantages and disadvantages of some different tomography methods.

### INTRODUCTION

ALICE is an energy-recovery linac-based electron accelerator currently operating with a maximum energy of 27 MeV, located at the STFC Daresbury Laboratory, UK. One of its functions is to provide a suitable beam to inject into the EMMA prototype non-scaling Fixed-Field Alternating-Gradient (ns-FFAG) accelerator, the first of its type in the world and currently in commissioning [1].

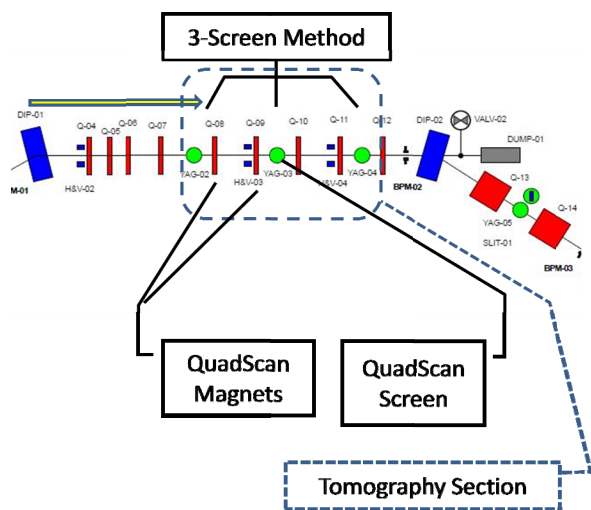


Figure 1: Schematic of part of EMMA injection line showing tomography section (beam from left).

When required, the ALICE beam is diverted by a dipole magnet into the EMMA injection line, which both transports the beam and matches it for injection into EMMA via a septum. In addition, the line has various diagnostics installed, including a phase-space tomography

section for ALICE beam characterisation, particularly prior to injection into EMMA.

The tomography section itself, shown in Fig. 1, consists of three fluorescent Yttrium Aluminium Garnet (YAG) screens, which can be moved into the path of the electron beam for imaging its transverse profile. These are separated by two pairs of quadrupole magnets, one horizontally focussing followed by one defocussing. A matching section of four quadrupoles, immediately preceding the first tomography screen, is used to adjust the beam's Twiss parameters as required.

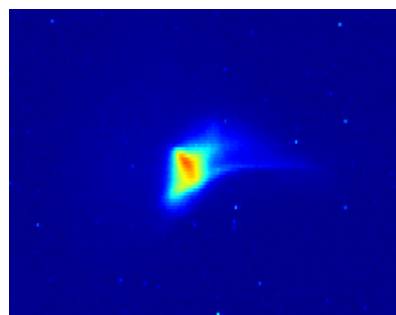


Figure 2: Typical screen image of beam (detail).

Tomography in phase-space depends upon underlying principles similar to conventional computed tomography in real space, as in medical X-ray CT [2]. A number of projections or views are obtained at incremental angles in a 180° range. When combined together using a reconstruction algorithm, information about an additional dimension is extracted; in real-space CT this gives a full 3-D volume, whereas in phase-space it is the  $x'$  dimension of the  $(x, x')$  distribution which is derived.

### TOMOGRAPHY METHODS

The ALICE configuration supports tomography by two distinct methods. The *three-screen* method uses the beam image on each of the three screens, giving a different projection angle corresponding to each of the three images. In contrast, the quadrupole scan method uses a range of quadrupole currents, generating a series of projections from images at a single screen downstream of the quadrupole. The choice of quadrupole/screen combination depends on: (a) the desired reconstruction location; (b) the optimum range of projection angles available; (c) the phase-space orientation to be studied (horizontal/vertical).

\*Work supported by the Science & Technology Facilities Council, UK.  
#mark.ibison@stfc.ac.uk

Although the three-screen method can in principle be applied directly, to obtain good results in practice it is necessary to adjust the quadrupoles in the matching section to get three good images at the design settings of the tomography section. Careful tuning can improve results if the corresponding spacing of the three projection angles is made roughly equal. To reconstruct the phase-space distribution from such a small projection set, the Maximum Entropy Technique is often used [3].

The *quadrupole scan* method, on the other hand, uses a set of quadrupole currents calculated to produce field gradients which give uniform angular projection intervals in phase-space at a subsequent screen [4].

The mathematical basis justifying tomographic reconstruction in phase-space has been covered elsewhere [5], but some of the main practical processing considerations will be discussed here.

(a) Preparation for Measurement.

The current-settings input file for the quadrupole scan is generated by software from parameters including beam energy, scan orientation (horizontal/vertical), beam-line configuration and magnet current limit. The current versus gradient calibration for the magnets has been measured for all quadrupoles by the manufacturer. The software also generates the set of transfer matrices corresponding to the current settings and projection angles.

(b) Data Acquisition.

With the desired screen in position – and others moved out of the beam – the scan is initiated and runs automatically. A computer file lists the required quadrupole currents. These are read one at a time to set the magnet current value and a corresponding camera image is captured. Because image capture is not synchronised to the beam repetition rate, individual images occasionally fail to capture the full beam intensity; an option for multiple captures per current value can be used to allow the software to save the brightest at each gradient. After completion of the scan, the image set is checked visually, and any failed exposures repeated by manually selecting the appropriate magnet current. This is aided by the file time-stamps which contain the screen and magnet identifiers and current setting.

(c) Post-Processing.

The raw image set undergoes several software processing stages to prepare it for reconstruction. The CCD cameras typically show a non-zero background noise level which is approximately constant across the image. One or more background images are used to calculate the mean level, which is subtracted from all beam images in the set. To correct for magnification differences between cameras, screen calibration factors (in mm/pixel) are applied. Images often contain non-beam artefacts such as spurious reflections; these may

be excluded by selecting a rectangular window around the beam on each image. The pixel intensities of each image are then scaled to give the same integrated intensities for all images, in order to correct for beam fluctuations. Projections are taken, either onto the x-axis for horizontal phase-space, or the y-axis for vertical phase space. In order to transform the projection to the reconstruction location, scaling factors are applied to projections and their corresponding positions arrays [5]. The centroid of each projection is calculated, for use by the reconstruction algorithm in compensating for any imperfect centring of the beam through the quadrupole.

(d) Reconstruction.

The sinogram, which is the array of projections ordered by angle, within the projections file is input to a Filtered Back-Projection (FBP) reconstruction code [2]; this generates a 2-D distribution in phase-space. Different sizes and resolutions of the reconstructed distribution can be generated.

## ANALYSIS TECHNIQUES

The accurate reconstruction of phase-space is always degraded by a number of effects: streak artefacts due to limited projection angles not covering the complete 0-180 degree range; irregularities in angle intervals; camera pixel noise in images. To reduce the effect of these imperfections on the parameters extracted from reconstructed distributions, several techniques are available.

(a) Filtering.

A simple median filter which replaces each pixel by the mean of its  $m \times n$  close neighbours will smooth out high-frequency noise. It should not be overdone if genuine small-scale features are to be retained. Zooming-in to a limited region of interest can also reduce the effect of noise in peripheral areas.

(b) Fitting.

The most radical processing option is to fit the raw reconstruction to a 2-D Gaussian function (surface fitting) by a least-squares method. It is assumed that in many cases a simple Gaussian will adequately describe the true distribution.

The three Twiss parameters  $\beta$ ,  $\alpha$ ,  $\gamma$  and geometrical emittance  $\varepsilon$  are related to the second moments of the distribution  $f(x, x')$  by:

$$\begin{aligned}\langle x^2 \rangle &= \beta\varepsilon \\ \langle xx' \rangle &= -\alpha\varepsilon \\ \langle x'^2 \rangle &= \gamma\varepsilon\end{aligned}$$

where

$$\varepsilon = \sqrt{\langle x^2 \rangle \langle x'^2 \rangle - \langle xx' \rangle^2}$$

Extraction of their values is therefore straightforward, although it is heavily influenced by the presence of noise in regions outside the main distribution centre. Estimates

obtained from distributions fitted according to (b) above do not have this problem.

## RESULTS OF EXPERIMENTS

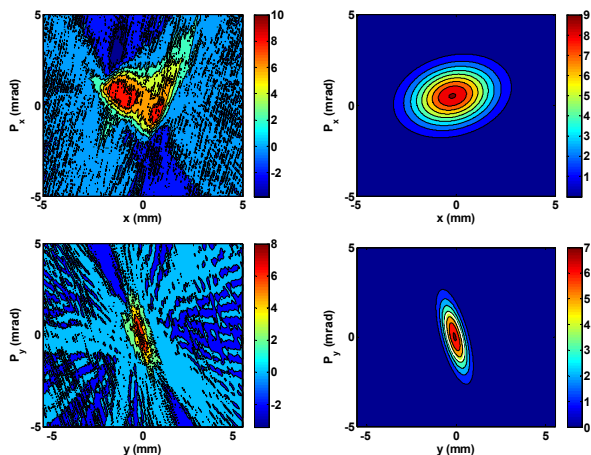


Figure 3: Reconstructed phase-space for 16.02.11 dataset: raw (L), fitted (R); horizontal (top), vertical (below).

Parameters derived from measurements made by scanning the same quadrupole (QUAD-08 & screen-02) under nominally identical beam conditions, operating the beam-line at an energy of 12MeV and bunch-charge of 40pC, have been compared. Measurements made on different dates are shown in Table 1.

Table 1: Summary of horizontal emittance  $\epsilon_x$  (geometrical) and Twiss parameters  $\beta$ ,  $\alpha$  derived from tomography measurements.

	$\epsilon_x$	$\beta_x$	$\alpha_x$
Date	(mm-mrad)	(m)	
16.02.11	1.51	1.31	-0.20
27.02.11	0.71	0.40	-0.96
09.03.11	0.67	0.38	-0.94

For horizontal phase-space, it is notable that the emittance and the Twiss parameters  $\beta$  and  $\alpha$  for the second two datasets agree well. The emittance estimate for the first measurement is however considerably larger. From the distribution (Fig. 3), phase-space appears as two distinct regions, possibly supporting the suggestion - from other measurements - of a split into sub-beams with different properties. Under these conditions, parameters derived from fitting a single Gaussian are unlikely to be meaningful.

Results after 16/02/11 show increased noise, ascribed to low image intensity due to the optical filtration introduced to reduce the risk of camera pixel saturation, which truncates the beam profile and so distorts the reconstructed distribution. This was necessary because the cameras used at present are a basic design (for robustness) and therefore lack features such as exposure control.

Comparisons with earlier horizontal emittance measurements  $\epsilon_x$  (Table 2) show broad agreement, especially in the case of the slit-scan<sup>‡</sup> and the simulation using the General Particle Tracer (GPT) assuming an elliptical cathode spot<sup>†</sup>, despite the difference in measurement conditions and positions (neglecting the 16/02/11 tomography data).

Table 2: Other methods [6] - Summary of emittance measurements/simulations. All values in mm-mrad.

Result	$\epsilon_x$	$\epsilon_y$
Single Slit	0.86	N/A
Slit Scan <sup>‡</sup>	0.72	N/A
Quad Scan	1.19	0.31
Measurement Average	0.92	0.31
GPT Simulation (Elliptical <sup>†</sup> )	0.75	0.15
GPT Simulation (Real Spot)	1.39	0.30

## CONCLUSIONS

We have used tomographic methods to reconstruct the horizontal and vertical phase-space distributions in the EMMA injection line. The results have been used to calculate the Twiss parameters and the transverse emittance of the beam. These will be of use in understanding the properties of the beam injected into EMMA, and in benchmarking existing models of the beam-line.

Further work on camera systems, to improve signal/noise ratios and optimise image intensity, is planned to increase confidence in parameters derived from the reconstructed phase-space.

Acknowledgement: The authors would like to thank Ben Shepherd for his help with the acquisition software.

## REFERENCES

- [1] R. Edgecock *et al.*, “EMMA: The World’s First Non-Scaling FFAG,” Proceedings of EPAC’08, Genoa, Italy.
- [2] A. C. Kak and M. Slaney, “Principles of Computerized Tomographic Imaging”, (SIAM, Philadelphia, USA, 2001), pp. 60-75.
- [3] K. M. Hock, “Tomography Reconstruction Codes: Maximum Entropy Technique (MENT)” <http://hep.ph.liv.ac.uk/~hock/tomography/MENT/ment.html>
- [4] K. M. Hock *et al.*, “Beam tomography in transverse normalised phase space“, Nuclear Instruments and Methods in Physics Research A (2011) doi:10.1016/j.nima.2011.04.002
- [5] C.B. McKee, P.G. O’Shea, J.M.J. Madey, Nuclear Instruments and Methods in Physics Research A 358 (1995) 764.
- [6] J. Garland, “Characterisation and Optimisation of the ALICE Accelerator as an Injector for the EMMA NS-FFAG”, Proceedings of IPAC’10, Kyoto, Japan.